AGRICULTURAL AND FOREST METEOROLOGY 149 (2009) 477–490

available at www.sciencedirect.com
ScienceDirect
journal homepage: www.elsevier.com/locate/agrformet

Reviewing SEBAL input parameters for assessing evapotranspiration and water productivity for the Low-Middle São Francisco River basin, Brazil
Part B: Application to the regional scale

A.H. de C. Teixeira [a,*], W.G.M. Bastiaanssen [b,c], M.D. Ahmad [d,e], M.G. Bos [f]

[a] Embrapa Semi-Árido, P.O. Box 23, 56302-970 Petrolina, PE, Brazil
[b] WaterWatch, Generaal Foulkesweg 28, 6703 BS, Wageningen, The Netherlands
[c] Delft University of Technology, Stevinweg 1, 2600 GA, Delft, The Netherlands
[d] International Water Management Institute, P.O. Box 2075, Colombo, Sri Lanka
[e] Currently at CSIRO Land and Water, GPO Box 1666, Canberra act 2601, Australia
[f] International Institute for Geo-Information Science and Earth Observations, P. O. Box 6, 7500 AA Enschede, The Netherlands

ARTICLE INFO

Article history:
Received 13 May 2008
Received in revised form
3 September 2008
Accepted 24 September 2008

Keywords:
Evapotranspiration
Biomass production
Water productivity
Remote sensing
Energy balance
Water management

ABSTRACT

The intensification of irrigated agriculture in the semi-arid region of Brazilian North-east results in a change of natural vegetation by irrigated fruit crops. New applications of remote sensing technologies are presented in this paper to estimate the impact of this land use change on regional water consumption – and ultimately the water balance – in Low-Middle São Francisco River basin. Ten Landsat images for a period from 2001 to 2007 were used, together with the locally calibrated Surface Energy Balance Algorithm for Land (SEBAL) and agro-meteorological data to derive information on regional actual evapotranspiration (ET), biomass production (BIO), and crop water productivity (CWP). The Landsat-based results revealed that regional mean ET for irrigated crops was 3.6 mm d^{-1} being higher than for natural vegetation (1.4 mm d^{-1}). Similar incremental ET values between natural and irrigated ecosystems were found from micro-meteorological field experiments. The consequence of this land use change on São Francisco River's downstream stream flow was assessed by estimating volumetric incremental evapotranspiration at the regional scale. The bio-physical crop water productivity per unit of actual evapotranspiration (CWP_{ET}) varied between 0.4 and 1.7 l of wine per m^3 of water for wine grapes; 1.7 and 4.0 kg of fruits per m^3 of water for table grapes; and 2.2 and 5.0 kg of fruits per m^3 of water for mangos. The accompanying paper (Part A) describes the calibration and validation of SEBAL steps witnessed under the actual field conditions in this study area.

1. Introduction

The São Francisco River crosses six Brazilian states, and has a basin size of approximately 636,920 km^2. A cropped area of 342,700 ha is irrigated. The average flow rate is 2850 $m^3 s^{-1}$ accounting for roughly two-thirds of the surface water resources in North-east Brazil.

The Low-Middle São Francisco sub-basin has an area of 115,987 km^2 (18.2% of the São Francisco River basin). The total irrigated area is 93,200 ha, which represents 27% of the irrigated

* Corresponding author. Tel.: +55 87 38621711; fax: +55 87 38621744.
E-mail address: heribert@cpatsa.embrapa.br (A.H. de C. Teixeira).

doi:10.1016/j.agrformet.2008.09.014

area of the total basin. The dominant vegetation cover in this sub-basin is ''caatinga'', a natural savannah area. The main commercial crops are irrigated vineyards and mango orchards. Water scarcity can potentially cause depletion of water resources resulting in aquifer mining and stream flow reduction. In addition, agricultural drainage and urban sewage deteriorate the water quality when excess water returns to the river system, both locally and further downstream. With increasing water scarcity and decreasing water quality, all water users (urban, industrial, agricultural, and ecological) are calling for an appropriate and fair share of the fresh water resources, even that the depletion of the water resources occurs productively.

Diversion of irrigation water is receiving a growing concern, because diverted water often is used with low efficiency and competition for water is increasing (e.g. Bos and Nugteren, 1974; Wolters and Bos, 1990; Bos et al., 2005). Irrigation thus should maximize crop water productivity by using the proper volume of water with sustainable water management (Bastiaanssen et al., 2008).

The professional and public debates of irrigation water diversions and water use efficiencies are often based on poor knowledge bases. As a minimum prerequisite, the discussions should be based on total volumes of net consumed water (i.e. diversion minus return flow) and the total goods that this consumption creates in terms of physical crop production and rural economic development. Hence, judgments on irrigated agriculture should be based on reliable data that have a regional perspective.

The challenge of the irrigation sector is to produce more food from less water. Water productivity (WP) reflects this challenge by exposing the ratio of the net benefits from crop, forestry, fishery, livestock and mixed agricultural systems to the amount of water consumed to produce those benefits (Sakthivadivel et al., 1999; Steduto et al., 2007). Crop water productivity (CWP) represents the fresh crops (in kg ha^{-1}) or benefits (in \$ ha^{-1}) produced per unit of water applied or consumed (in m^3 ha^{-1}). It is recommended to analyze the CWP in terms of actual evapotranspiration (ET) because this indicator also includes non-irrigation water, such as rainfall, capillary rise, and soil moisture changes (e.g. Droogers and Kite, 1999). These water resources also contribute to crop production, and thus CWP cannot be related to irrigation water supply only.

Benchmark values for water productivity of irrigated crops (wheat, rice, cotton, maize) were summarized by Zwart and Bastiaanssen (2004); for dryland crops by Oweis and Hachum (2006) and for rainfed crops by Rockstrom and Barron (2007). Literature on crop water productivity in fruit crops is still scarce. Some related papers can be found in Goodwin and O'Connell (2008).

In semi-arid and arid regions, water use of irrigated crops exceeds that of natural rainfed ecosystems reducing the downstream stream flow. Nowadays, the magnitude of this effect can be analyzed by satellite remote sensing data, quantifying the spatial and temporal variation of ET in composite landscapes (e.g. Kustas et al., 2004; Allen et al., 2007a,b). For instance, Bastiaanssen and Chandrapala (2003) and Morse et al. (2004) developed relationships between land use classes and their ET volumes for basins in Sri Lanka and Idaho (US).

The first objective of this paper is to demonstrate that satellite measurements, combined with agro-meteorological data, can be used to determine evaporative depletion and biomass production for irrigated land and natural vegetation. The second objective is to quantify the net water withdrawals in Low-Middle São Francisco River basin by assessing: (i) the incremental evapotranspiration between natural vegetation and irrigated crops and (ii) the crop water productivity for understanding whether the extra water is consumed productively.

2. Materials and methods

The field experiments with wine grape were carried out at Vitivinícola Santa Maria farm, near the town of Lagoa Grande (Lat. 09°02′S; Long. 40°11′W), in Pernambuco state. The cultivar was *Petite Syrah*, with 10 years old at the start of the measurements in 2001. Because the grapes were pruned two times during 2002 for wine production, the water productivity analyses involved two growing seasons (GS1 and GS2) in that year. The duration of GS1 was 132 days, from 7 February to 19 June 2002, while the GS2 comprised 136 days, from 8 July to 22 November 2002.

The field experiments with table grape were in Vale das Uvas farm near the town of Petrolina (Lat. 09°18′S; Long. 40°22′W), Pernambuco state. The cultivar was *Superior Seedless*, 2 years old in 2002. Two growing seasons with 90 days duration each one were from 8 July to 7 October, in 2002 and in 2003, but only the second one (GS2) yielded fruits for CWP analyses. Details of the instruments used in both vineyards are described by Teixeira et al. (2007).

The mango orchard experiments for CWP analyses involving two growing seasons (GS1 and GS2) were with the cultivar *Tommy Atkins*, 18 years old (in 2003), in the Fruitfort farm, near the town of Petrolina (Lat. 09°22′S, Long. 40°34′W), Pernambuco state. Two growing seasons (GS1 and GS2) were used for CWP analyses. The duration of GS1 was 390 days, from 1 October 2003 to 24 October 2004. The measurements continued into a second period of 370 days, from 25 November 2004 to 29 November 2005 (Teixeira et al., 2008a).

The flux tower in caatinga (i.e. natural bush land vegetation) was located at 09°03′S and 40°19′W, near the town of Lagoa Grande, Pernambuco state. Two years (2004 and 2005) were used for incremental evapotranspiration and biomass production analyses (Teixeira et al., 2008b).

Satellite-based computations of ET were performed with Landsat Thematic Mapper (TM) cloud-free satellite images (path/row 217/66). The images were acquired in 10 September 2001, 4 October 2001, 6 July 2003, 24 September 2003, 12 October 2004, 14 November 2004, 15 October 2005, 16 November 2005, 30 July 2006 and 22 January 2007. The total period was from 2001 to 2007 covering different months of the years and growing seasons. The Landsat satellite overpass is approximately at 09:30 local time. The TM bands 1–5 and 7 provide reflectance data for the visible and near infrared radiation in pixel sizes of 30 m × 30 m. TM band 6 measures longwave (thermal) radiation. The pixel size for this last band is 60 m × 60 m for Landsat 7 and 120 m × 120 m for Landsat 5.

Interpolated weather data from seven automatic agrometeorological stations were used for the calculations of the surface energy balance terms using the SEBAL algorithm and regional reference evapotranspiration (ET_0) data. The interpolation of the ET_0 point data was done by the "moving average" method. The stations are equipped with weather data for the calculation of ET_0 by the FAO Penman–Monteith method (Allen et al., 1998). The automatic agro-meteorological stations and satellite images are described in the accompanying paper (Part A).

The set of individual equations tested in the accompanied paper (Part A) were used to derive the complete radiation and energy balances pixel-by-pixel. The daily actual evapotranspiration (ET_{24}) was obtained by multiplying instantaneous values of the evaporative fraction (EF_{inst}) by a 24 h value of net radiation (R_{n_24}) and a correction term a:

$$ET_{24} = a EF_{inst} R_{n\_24} \quad (1)$$

where a = 1.18 is the regression coefficient from the relationship between EF_{inst} and daily values of evaporative fraction (EF_{24}). The instantaneous (subscript inst) and daily (subscript 24) evaporative fractions were calculated by

$$EF_{inst} = \frac{\lambda E_{\_inst,24}}{R_{n\_inst,24} - G_{inst,24}} \quad (2)$$

where λE, R_n and G are the latent heat flux, net radiation and soil heat flux, respectively. R_{n_24} was acquired applying the locally calibrated Slob equation (Teixeira et al., 2008b).

The interpolated daily values of the reference evapotranspiration (ET_{0_24}) yielded a grid of reference data. Following Allen et al. (2007a,b), the annual (subscript year) or seasonal (subscript GS) actual evapotranspiration ($ET_{\_Year,GS}$) were calculated with the reference evapotranspiration for these time scales ($ET_{0\_Year,GS}$) as

$$ET_{\_Year,GS} = \left(\frac{ET_{24}}{ET_{0\_24}}\right)_{avg} ET_{0\_Year,GS} \quad (3)$$

where $(ET_{a\_24}/ET_{0\_24})_{avg}$ are the calibrated and averaged daily ratios for the year or growing season (GS). The limited availability of cloud free Landsat images is the main argument for using Eq. (3) as a simplified method to estimate annual or seasonal regional evapotranspiration including natural vegetation and irrigated land.

The calculation of CWP, based on actual evapotranspiration, requires ET and biomass production (BIO) for a growing season. BIO is obtained from photosynthetically active radiation (PAR) and light use efficiency (ε) for specific type of vegetations. The flowchart is shown in Fig. 1.

Because the accompanying paper (Part A) does not show the theoretical aspects of BIO, a few major equations are provided here. The interpolated daily global solar radiation values for 24 h (RG_{24}) were used to estimate the regional photosynthetically active radiation for the same time scale (PAR_{24}):

$$PAR_{24} = b\, RG_{24}\, (W\, m^{-2}) \quad (4)$$

where b = 0.44 is the constant of the regression equation that reflects the portion of total solar radiation that can be used for photosynthesis (Teixeira et al., 2008b). The values of the absorbed photosynthetically active radiation for 24 h ($APAR_{24}$) were directly approximated from PAR_{24}:

$$APAR_{24} = f\, PAR_{24}\, (W\, m^{-2}) \quad (5)$$

The factor f (i.e. $APAR_{24}/PAR_{24}$) was estimated from NDVI (e.g. Asrar et al., 1984). Bastiaanssen and Ali (2003) considered for a mixture of arable crop types the following coefficients:

$$f = -0.161 + 1.257 NDVI \quad (6)$$

The annual (subscript Year) and seasonal (subscript GS) accumulated biomass productions were obtained as

$$BIO_{Year,GS} = \sum (\varepsilon_{max} EF\, APAR 0.864)\, (kg\, ha^{-1}) \quad (7)$$

where ε_{max} is the maximum light use efficiency, which according to Monteith (1972) varies only with c3 and c4 crops (if not water stressed). In the present study ε_{max} was considered 2.5 g MJ^{-1}, which is an average value for c3 crops found in the literature (Bastiaanssen and Ali, 2003). The improvements of Monteith's model have resulted in correction terms for environmental conditions; including soil moisture and heat stresses (e.g. Field et al., 1995). In the actual study only the correction scalar for water stress was computed by EF (Bastiaanssen and Ali, 2003) as the region does not present thermal restriction to the crop growth.

The CWP in three representative farms was expressed in this paper as fruit and wine productions per cubic meter water consumed (Teixeira et al., 2007, 2008a):

$$CWP_{ET} = \frac{BIO_{GS}}{ET_{GS}} AHI\, (kg\, m^{-3} \text{ or } L\, m^{-3}) \quad (8)$$

where AHI is the apparent harvest index required for the conversion of total dry matter into fresh yield. In this case study, AHI values were acquired by dividing fresh fruit productions measured by the farmers for the growing seasons by BIO_{GS} from satellite images for three representative farms of grapes and mangos, in the plots where the flux towers were installed and the production of fruits were measured for the growing seasons. This ensures that the proper average fruit yield at the farm can be derived from remote sensing; the interest is in the spatial variation across the farm. For wine grapes the fruit yields were converted in wine productions, by considering that 1.25 kg of grapes yielded 1 l of wine (Teixeira et al., 2007).

The satellite values of ET_{24}/ET_{0_24}, EF_{24} and NDVI were calibrated with field measurements in irrigated crops (Teixeira et al., 2007, 2008a) and natural vegetation (Teixeira et al., 2008b). After calibrations and interpolations of satellite images, the annual and seasonal values of ET and BIO were obtained using Eqs. (3) and (7), respectively. The three representative commercial farms of wine grapes, table grapes and mangos were analyzed in terms of CWP.

3. Results and discussion

3.1. *Energy partitioning*

The 24 h energy partition was expressed by Eq. (2) taking G_{24} zero for this time scale. The EF_{24} for three different periods of the year (before, just after, and during the rainy season) are presented in Fig. 2.

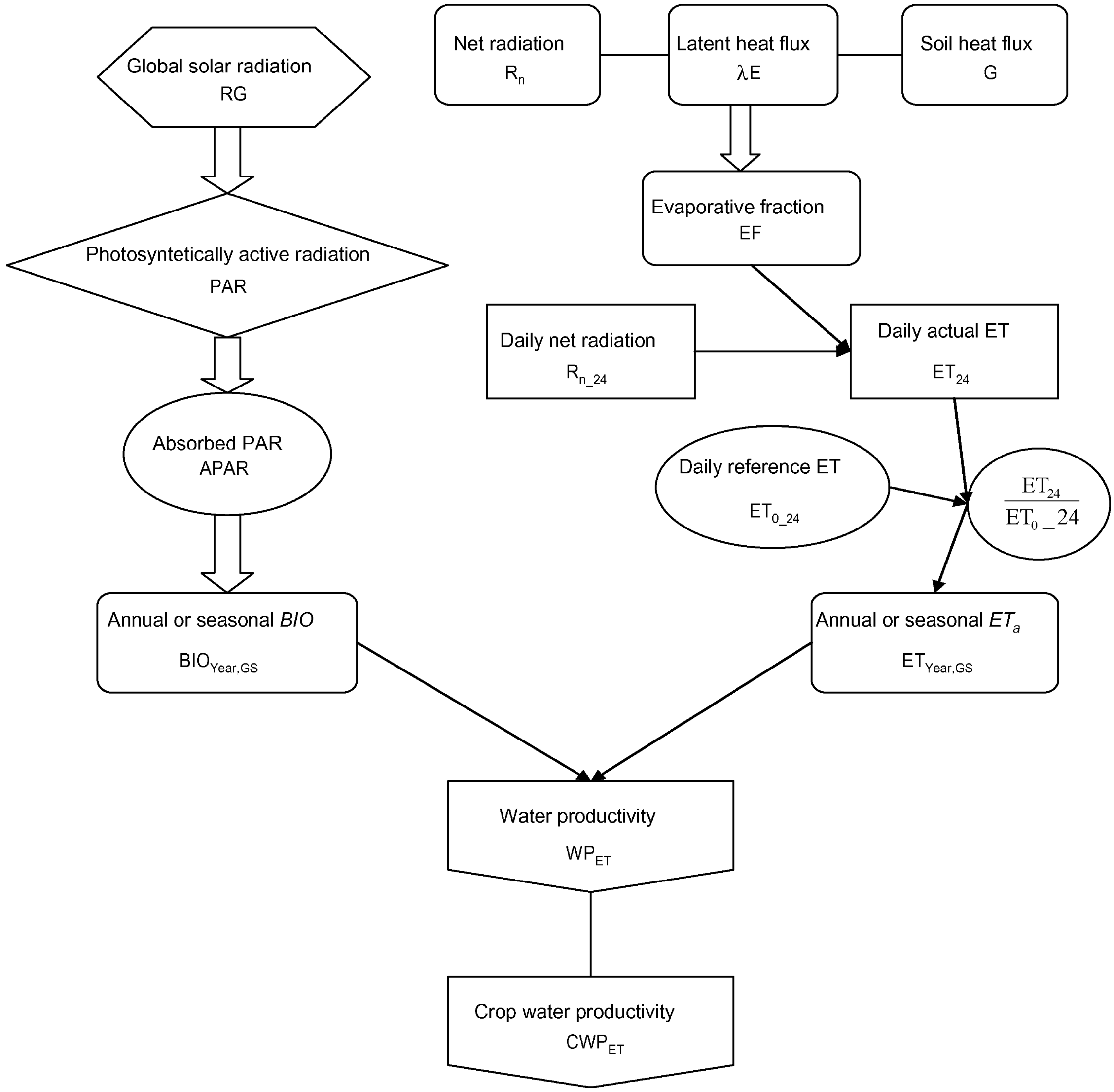

Fig. 1 – Schematic flowchart for calculation of bio-physical crop water productivity (CWP_{ET}).

The natural vegetation (caatinga) converted large portions of the available energy into sensible heat flux (*H*), causing values of H_{24}/R_{n_24} higher than 0.90 during the driest period of the year (October–November), while the irrigated agricultural fields presented high values of $\lambda E_{24}/R_{n\_24}$. In general, irrigation intervals were small during this period (daily irrigation), and the water supply was rather uniform reducing heat losses to the atmosphere. As a consequence, values of EF_{24} for irrigated crops were near 1.00, while for caatinga this indicator varied from 0.00 to 0.20 (Fig. 2a).

EF_{24} had intermediate values just after the rainy season, because antecedent precipitation during January to April provided sufficient water storage in the caatinga root zone still keeping this natural ecosystem wet and green, despite the quick rise of the atmospheric demand (Fig. 2b). During this period EF_{24} in natural vegetation reached to 0.35, while irrigated crops presented values about 0.80.

During the rainy season, the evapotranspiration rates from caatinga were – in some cases – similar to those from irrigated areas. A high portion of the daily available energy in natural vegetation was converted into λE_{24} (Fig. 2c), making the values of EF_{24} around 0.50 for both kind of vegetation as the most of the farmers stopped irrigation during this period and rainfall kept the soil wet for all ecosystems.

Bastiaansssen (2000) found similar EF_{24} values for irrigated cotton and perennial vegetation (vineyards and orchards) varying from 0.40, when the crops started to be irrigated to 0.70–0.90 during the irrigation season in Gediz basin (Turkey). Li et al. (2006) reported that for a grazing steppe in central Mongolia, seasonal values of EF_{24} followed the variation in leaf areas and rainfall events during the dry–wet cycles, similar with the results for natural vegetation in Brazilian semi-arid region. Farah et al. (2004) showed EF_{24} values of 0.70 during the wet season and 0.10 during the dry season, for a tropical watershed in the Kenyan Rift Valley with natural meadows. The magnitudes of the energy partitioning in the actual study were thus plausible.

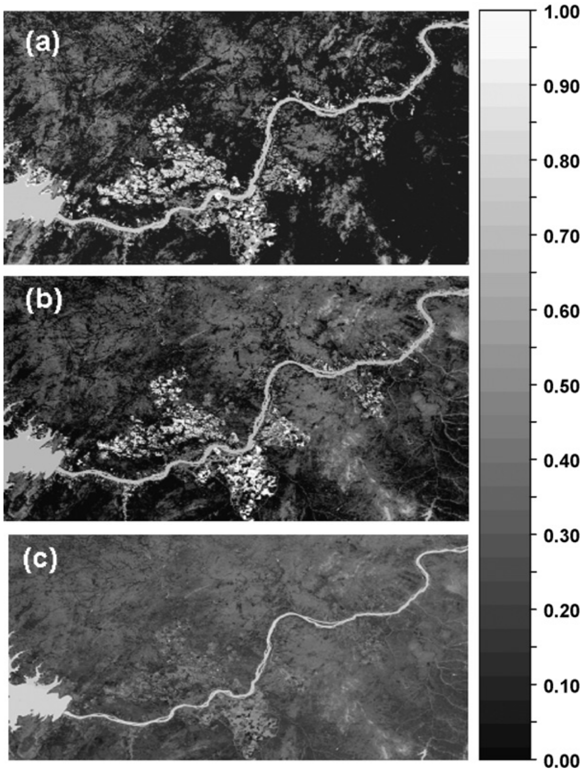

Fig. 2 – Daily energy partition ($EF_{24} = \lambda E_{24}/R_{n\_24}$): for the dry season in October of 2005 (a); for the end of the rainy season in June of 2006 (b) and for the rainy season in January of 2007 (c).

3.2. *Regional actual evapotranspiration*

Fig. 3 presents the histograms for daily ET values in the semi-arid region of the Low-Middle São Francisco sub-basin. The averaged values for the 10 individual days in different years and growing seasons are shown. The Landsat pixels were divided in classes of irrigated and natural vegetation lands to highlight the incremental ET due to irrigation by using a simplified multi-spectral classification.

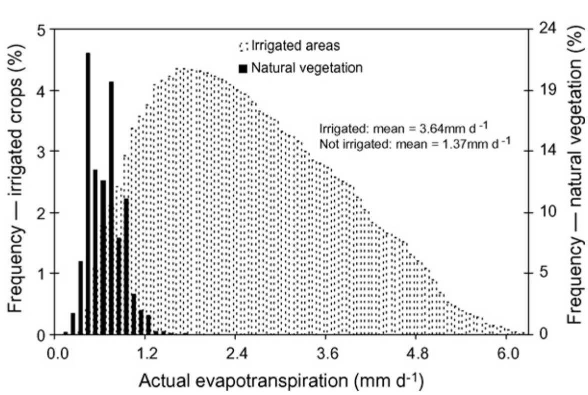

Fig. 3 – Histograms of daily ET for irrigated and non-irrigated areas averaged according to the 10 Landsat TM images acquired during different moments of the growing seasons and across different years.

The effect of soil moisture was strong during the dry season. Pixels with ET lower than 1 mm d^{-1} occurred frequently during this condition. These pixels represent natural vegetation (caatinga). The distribution of ET in caatinga was more skewed and tended towards the lowest values. Values of 1.0–5.0 mm d^{-1} coincided with irrigated crops, mainly table grapes. While the average value for all irrigated areas was 3.6 mm d^{-1}, natural vegetation had a mean value of 1.4 mm d^{-1}. Irrigated crops thus evaporated around 2.2 mm d^{-1} more than caatinga.

Landsat images for the dry seasons of 2004 and 2005 (October and November) were integrated with those representing the wet seasons of 2006 (June) and 2007 (January) to derive annual ET values. The regression equations of ET/ET_0 between field data of 2004 and 2005 and satellite values involving the period 2001–2007 and the same day of the year (DOY) for irrigated mango orchard and natural vegetation were applied (Fig. 4) to calibrate the images of 2006 and 2007. After calibration, successive interpolations were performed to retrieve the monthly values of ET/ET_0 for 2004 and 2005 and then the annual values. The mean annual values for this ratio of these years were averaged for calculating the average regional annual ET by using the grids of ET_0 and Eq. (3) (Fig. 5). Although this is a simple method to obtain averaged annual values, it is probably the best possible way to assess time integrated regional scale ET at high resolution for different land use classes in Low-Middle São Francisco River basin.

The highest accumulated regional ET values were found for table grapes, being around 800–1300 mm $year^{-1}$. Mango orchards had lower values than vineyards, ranging from 600 to 1100 mm $year^{-1}$ while in caatinga they were between 200 and 600 mm $year^{-1}$. The values for natural vegetation were close to the amounts of annual rainfall.

The total rainfall in 2004 was 720 mm, above the long-term value of 570 mm $year^{-1}$. The year 2004 was thus exceptionally wet. The year 2005 was a dry year with 337 mm of rainfall. The average conditions of these two years were considered representative for a long-term condition.

Caatinga has the ability of turning into a verdant green ecosystem during the rainy season. By the end of this wet period, natural vegetation showed moderately high values of ET/ET_0 ($\sim$0.30–0.35) due to the ability of the roots in using soil moisture from deeper layers and in conserving this water.

3.3. *Incremental evapotranspiration*

The monthly and annual SEBAL results of ET in conjunction with field measurements are shown in Table 1. The total annual ET from satellite measurements for caatinga during 2004 was with 644 mm slightly lower than the measured rainfall (720 mm). The annual ET for the year of 2005 in caatinga was much lower (376 mm), but slightly higher than the measured rainfall (337 mm). This suggested that during dry years, bush lands extract moisture from the soil profile that is stored during preceding wetter years.

The difference between estimations of ET based on satellite data and the field measurements for natural vegetation in 2004 was only 4.7%. For the second year in 2005, this difference reduced to 4.1%. The significantly lower ET of caatinga during 2005 as compared to 2004 agreed well with the reduction of rainfall. For mango orchard, the differences between SEBAL and

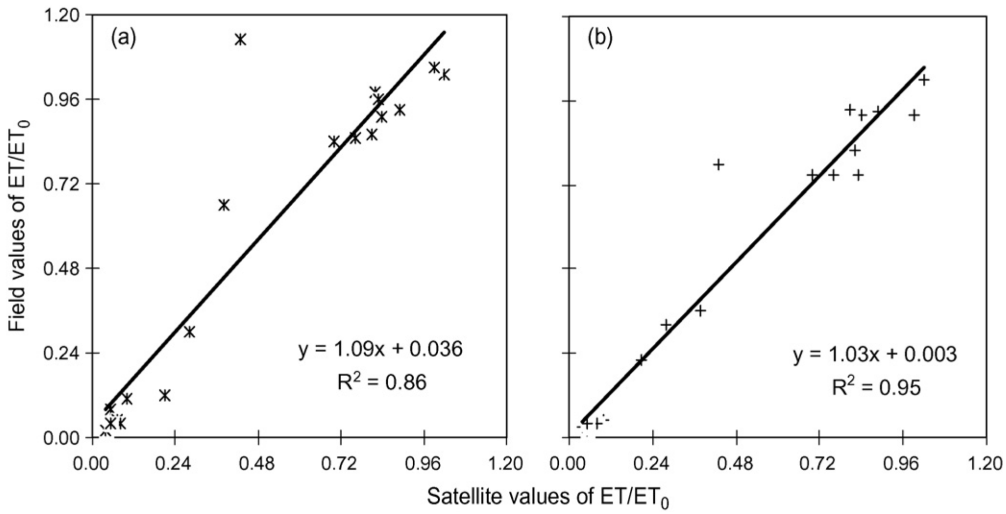

Fig. 4 – Relationship between the field and satellite values of ET/ET_0 for irrigated mango orchard and natural vegetation. Values from images involving the period 2001–2007 were compared with field data for 2004 (a) and 2005 (b) with the same day of the year (DOY).

field measurements were 0.6% and 0.5% only, for 2004 and 2005, respectively (Table 1). The magnitudes of these differences after calibrations are better than earlier validation reports of SEBAL where they pointed that accumulated ET values can be estimated with 95% accuracy (Bastiaanssen et al., 2005).

Since caatinga showed an ET of 644 mm and mango orchard 1445 mm in 2004, the increment is 801 mm or a factor 2.24. For 2005, this difference between 376 mm (caatinga) and 1232 mm (mango orchard) is 856 mm, or a factor 3.27. Hence, it can be concluded that irrigated mango orchards evapotranspirate more than double the amount for caatinga in a year and that the incremental ΔET on average is 828 mm $year^{-1}$.

Some summary statistics of land use and ET for the Low-Middle São Francisco River basin are given in Table 2. The mango orchards and vineyard areas represent 20% and 9% of the total irrigated area, respectively, with a total evaporative depletion of 0.36 km^3 $year^{-1}$. Because the incremental ΔET for

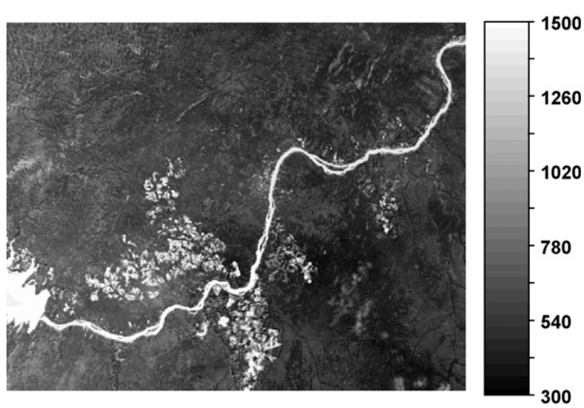

Fig. 5 – Averaged annual ET for the region comprised by the net of agro-meteorological stations in Low-Middle São Francisco River basin. Monthly field values of ET and ET_0 for 2004 and 2005 were used for calibration of satellite counterparts.

the first crop is 2.2 mm d^{-1} and for vineyards it is 2.5 mm d^{-1}, the additional volume of water used for ET in these two main irrigated fruit crops in the sub-basin is around 0.22 km^3 $year^{-1}$. For all irrigated crops, the total evaporative depletion increases to 0.75 km^3 $year^{-1}$ (93,180 ha and ΔET of 2.2 mm d^{-1}). The latter volume represents the net depletion; the difference between diversion and return flow that is truly consumed and not longer available for downstream urban and environmental users.

In an earlier study in the Nilo Coelho area (Bastiaansssen et al., 2001), in the Low-Middle São Francisco River basin, ET outside the irrigated areas was 70% of the annual rainfall. The total ET for irrigated fruit crops resulted in 0.15 km^3 $year^{-1}$, while the rainfall totaled 0.08 km^3 $year^{-1}$ in these plots. The ET due to rainfall was then 0.06 km^3 $year^{-1}$. The resulting incremental ET (0.09 km^3 $year^{-1}$) was 60% of the amount that is diverted from the Sobradinho reservoir. Applying this percentage to the actual net withdrawal of 0.75 km^3 $year^{-1}$ the amount diverted from the river was estimated as 1.25 km^3 $year^{-1}$. Assuming that 80% of the losses – i.e. the difference between diversion and ET – are recaptured back into the river, the net withdrawal from the river becomes 0.85 km^3 $year^{-1}$ with a return flow of 0.40 km^3 $year^{-1}$ and 0.10 km $year^{-1}$ being seepage to deep aquifers.

3.4. *Water productivity*

Irrigated crops in semi-arid Brazil produce large amounts of biomass as a result of the effects of abundant solar radiation, favourable air temperature and moist soils during the irrigation periods and rainy seasons. The PAR during October and November is very high and this radiation is intercepted by the crop leaves for photosynthesis and dry matter production. The natural vegetation (caatinga) is only green during the rainy periods. The contrast between caatinga and irrigated ecosystems becomes apparent when analyzing the regional distribution of biomass production.

Table 1 – Monthly actual ET from field and satellite measurements for irrigated crop – mango orchard (MG) and natural vegetation – caatinga (CT), together with monthly rainfall amounts during the years of 2004 and 2005. The field data represent point values. The satellite data are a reflection of thousands of pixels.

Year/Month	MG_Field (mm)	CT_Field (mm)	MG_Satellite (mm)	CT_Satellite (mm)	Rainfall (mm)
2004					
January	104.6	100.9	104.0	94.2	397.8
February	118.7	131.1	118.6	123.8	187.0
March	128.1	130.3	127.7	124.6	61.2
April	125.7	104.9	125.9	99.7	13.5
May	107.3	70.8	107.8	68.7	29.7
June	97.8	37.7	97.8	36.0	6.1
July	102.2	24.3	113.1	26.4	0.8
August	114.7	15.0	115.5	14.3	0.5
September	141.4	10.9	142.0	10.0	0.8
October	140.3	9.8	140.9	9.5	1.5
November	130.1	17.2	126.4	15.4	20.3
December	125.7	23.2	125.2	20.9	0.5
Year	1437	676	1445	644	720
2005					
January	116.2	69.5	116.2	64.6	48.5
February	103.2	63.4	103.5	62.4	78.0
March	115.2	82.2	114.2	78.4	89.9
April	110.7	44.1	110.0	42.4	24.4
May	89.9	32.0	92.8	32.2	2.0
Jun	97.7	28.5	94.7	26.7	31.5
July	105.8	30.3	105.0	29.6	2.8
August	110.5	7.2	110.3	6.7	1.3
September	111.3	3.6	113.2	3.0	0.0
October	108.6	6.5	111.8	6.8	0.0
November	78.4	6.6	81.6	6.0	26.9
December	78.8	18.5	79.1	17.6	31.8
Year	1226	392	1232	376	337

To use Eq. (7), the values of EF were calibrated and interpolated in the same was as for ET/ET_0 applying the regression equations of Fig. 6 to the images of 2006 and 2007. To calculate APAR for the same period, NDVI values of the images of 2006 and 2007 were calibrated using the regression equation between this vegetation index and field values of daily surface albedo for 2004 and 2005 (Fig. 7). After that, the estimated field values of NDVI were correlated with satellite values in the same way as it was for ET/ET_0 and EF (Fig. 8). The regression equations were applied to the images of 2006 and 2007. After the successive interpolations of values of EF and APAR, the annual values were used to estimate the total biomass production (BIO_{Year}) by Eq. (7) (Fig. 9). The combination of pixel values of 2004 (above long-term rainfall) and 2005 (below long-term rainfall) gave average conditions.

The most frequent BIO_{Year} values for all ecosystems were in the range of 14.0–34.0 t ha^{-1}. The highest values were found in irrigated mango orchards (50–100 t ha^{-1}) and vineyards (30–100 t ha^{-1}). As for BIO_{year}, to calculate BIO_{GS} the same procedure of calibration and interpolation was done for the growing seasons of wine grapes (2002), table grape (2003) and mango orchard (2003–2005). The regression analyses between field and satellite values of ET/ET_0, EF and NDVI are shown in Fig. 10. These equations were applied to the images for different years but with the DOY inside the period of the growing seasons.

By combining yield data of wine grapes, table grapes and mango orchards from farmer measurements and satellite estimates of accumulated biomass production for the growing seasons (BIO_{GS}), the apparent harvest indices (AHI) were obtained (Table 3). The AHI describe the ratio of fresh yields to

Table 2 – Main land cover types, area and averaged daily and annual actual evapotranspiration in Low-Middle São Francisco basin from field and SEBAL measurements.

Surface type	Area (ha)	Area (%)	ET_{24} (mm d^{-1})	ET_{Year} (km^3 $year^{-1}$)
Vineyards	8,180	9	3.9[a]	0.12
Mango orchards	18,607	20	3.6[b]	0.24
Irrigated crops	93,180	100	3.6[c]	1.22
Not irrigated	11,505,520	–	1.4[c]	58.79

[a] *Source*: Teixeira et al. (2007).
[b] *Source*: Table 1.
[c] *Source*: Landsat images of Fig. 3.

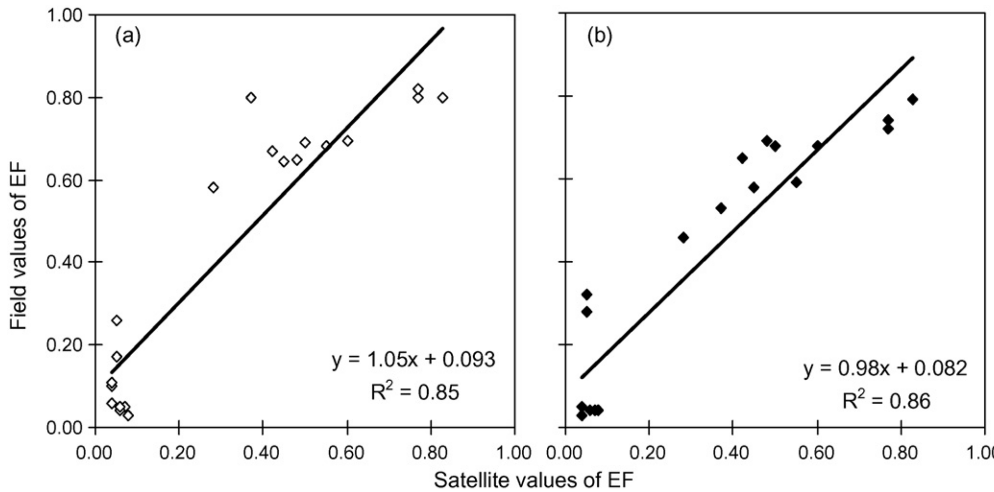

Fig. 6 – Relationship between the field and satellite values of EF for irrigated mango orchard and natural vegetation. Values from images involving the period from 2001 to 2007 were compared with field data for 2004 (a) and 2005 (b) with the same DOY.

the total produced dry matter. The AHI values were subsequently applied to the three representative commercial farms of wine, grapes and mangos, where the flux towers were. The main reason for the higher values of AHI for mangos is due to the size of the fruits that increases the physical values of production.

3.5. *Crop water productivity*

3.5.1. *Wine grapes*

The CWP_{ET} maps for wine grapes, as well as the histograms for the two growing seasons (GS1 and GS2) in Vitivinícola Santa Maria farm, are shown in Fig. 11. The crop water productivity analyses were done in terms of wine.

For GS1, irrigated wine grapes presented CWP_{ET} values between 0.40 and 0.80 L m^{-3} for 98% of pixels. The average was 0.60 L m^{-3} (i.e. 0.75 kg m^{-3} of water consumed) with a standard deviation (std) of 0.22 L m^{-3}. For GS2, 90% of the pixels were in the range from 0.70 to 1.70 L m^{-3} averaging 1.15 L m^{-3} (i.e. 1.44 kg m^{-3} of water consumed) and a std of 0.40 L m^{-3}. The average coefficient of variation (CV) for the two seasons was 32%. When the crop water productivity was based on actual transpiration—CWP_T (Teixeira et al., 2007), the averaged values for the two growing seasons became 0.69 and 1.29 L m^{-3} (i.e. 0.86 and 1.61 kg m^{-3}).

The differences in CWP values of bottled wine between GS1 and GS2 could be explained by the bio-physical processes. GS1 was cloudier and the duration of flowering and maturation of fruits stages were shorter than for GS2. The lower std in GS1 could be ascribed to more uniformity with respect to the crop stages than for GS2.

Considering CWP_{ET} defined as weight of fruits, Jarmain et al. (2007) found higher values in South Africa (4.70 kg m^{-3}). Walker et al. (2004) reported CWP_T of wine grapes (Shiraz and Cabernet) in Australia in the range from 2.50 to 3.30 kg m^{-3} under well-watered conditions, and from 2.00 to 5.10 kg m^{-3} under mild water deficit.

The economic value of wine depends on the registration and recognition of the brand name. Well established brands have a substantial higher price than ordinary wines. Considering the average price of 0.91 US\$ L^{-1} for the Shiraz wine in 2002 and in the study region, the corresponding monetary values of crop water productivity based on actual evapotranspiration ($CWP_{\$\_ET}$) ranged from 0.36 to 1.55 US\$ m^{-3}.

It can be concluded that the values of CWP in the present study for wine grapes are relatively low compared to those found in literature, showing the scope for improvement.

3.5.2. *Table grapes*

The CWP_{ET} map for table grapes together with the histogram for the second growing season (GS2) in Vale das Uvas farm is shown in Fig. 12. 99% of the values were between 1.70 and 4.00 kg m^{-3}, averaging 2.80 kg m^{-3} with a std of 1.00 kg m^{-3}. The CV is also high (36%) as in the case of wine grapes, what showed relatively large spatial variations for both vineyards. When the crop water productivity is based on actual

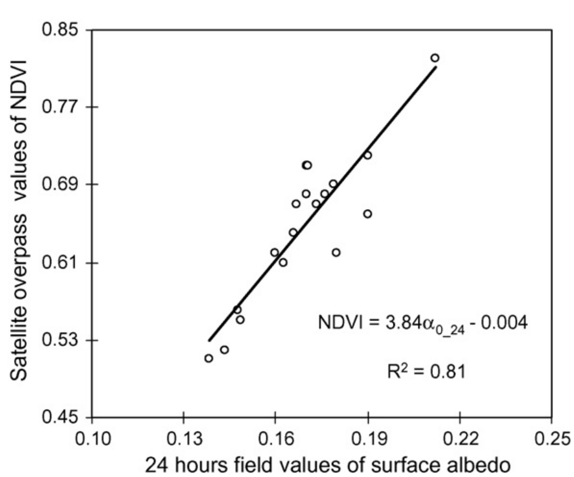

Fig. 7 – Relationship between satellite overpass values of NDVI and 24 h field values of surface albedo (α_{0_24}) for irrigated crops and natural vegetation.

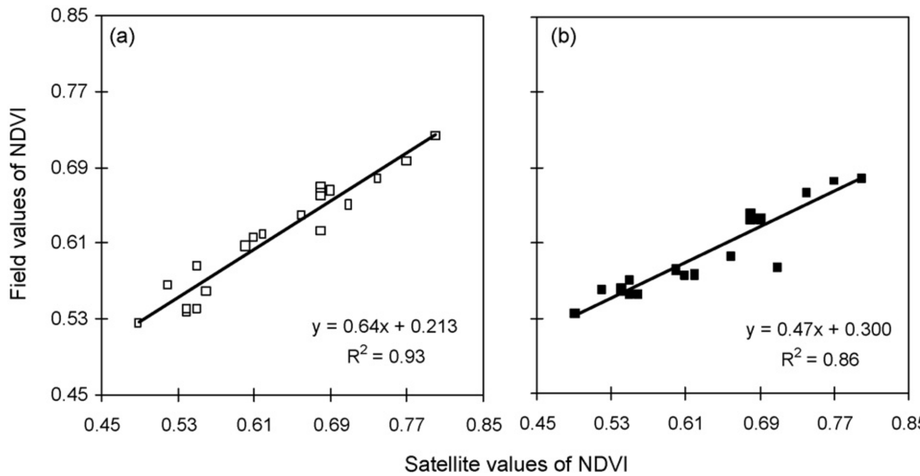

Fig. 8 – Relationship between the field and satellite values of NDVI for irrigated mango orchard and natural vegetation. Values from images involving the period from 2001 to 2007 were compared with field data of 2004 (a) and 2005 (b) with the same DOY.

transpiration (Teixeira et al., 2007) the CWP_T values were in the range from 2.04 to 5.17 kg m^{-3}. These results reflected the message that more uniformity on CWP is desirable.

The physical values of CWP for table grapes in the current study are lower than those found in Australia under drip (Yunusa et al., 1997a) and furrow irrigation (Yunusa et al., 1997b). In this last country, CWP_{ET} of drip irrigated table grapes were 8.60 kg m^{-3} for Grafted and 4.30 kg m^{-3} for Own-rooted vineyards, while CWP_T were 16.50 and 11.50 kg m^{-3}, respectively. In the furrow irrigated grapes, CWP resulted in 1.33 and 4.05 kg m^{-3} when based on ET for two different growing seasons, respectively, corresponding to a CWP_T of 8.40 and 21.11 kg m^{-3}. Klaasse et al. (2007) and Jarmain et al. (2007) reported a mean value CWP_{ET} of 3.70 kg m^{-3} for table grapes in South Africa.

The lower Brazilian values of vineyards CWP are related to the lower yields associated with higher daily water consumptions. Teixeira et al. (2007) discussed that although the CWP_{ET} and CWP_T values for one growing season in Low-Middle São Francisco River basin are lower than in regions where the climate is temperate, the total production of 2.5 growing seasons compensate these differences and for 1 year the total yield is in good agreement with, for instance, South Africa and Australia (but the total water consumption in these last countries is substantially higher). One of the reasons for significant non-uniformity in vineyards is the presence of multiple varieties with different crop stages and cultural management practices. Nevertheless, the variations are high when compared with for instance wheat (Zwart and Bastiaanssen, 2007) that had a CV of typically 14% (ranging from 5% to 30%).

As the growing season of seedless table grape (3 months) is shorter than that for wine grape (4 months) in Low-Middle São Francisco River basin; the seasonal ET for wine grapes was higher, contributing to a lower CWP values among other factors. However, the difference between CWP_{ET} and CWP_T was higher for micro-sprinkler irrigated table grapes than for the drip irrigated wine grapes, reflecting the better perfor-

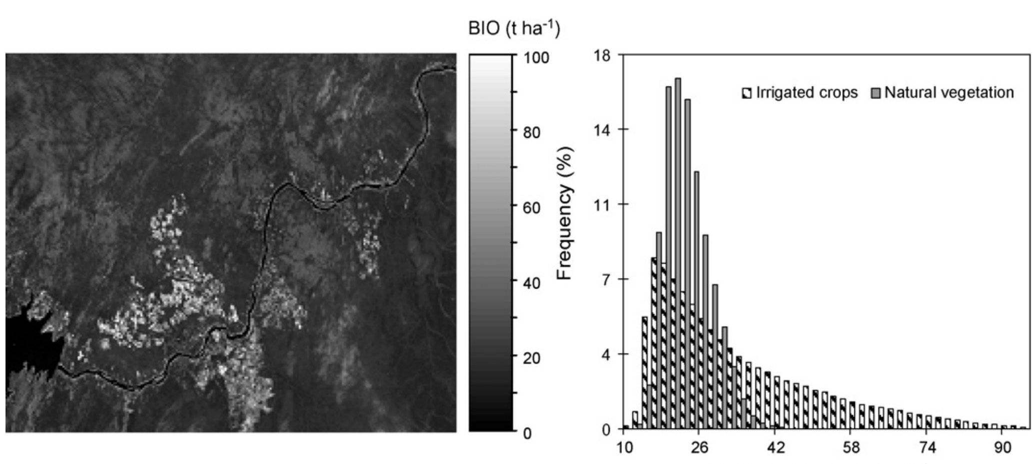

Fig. 9 – Map (a) and histograms (b) of mean annual total biomass production (t ha^{-1}) averaged for 2004 (wet year) and 2005 (dry year) in the Low-Middle São Francisco River basin.

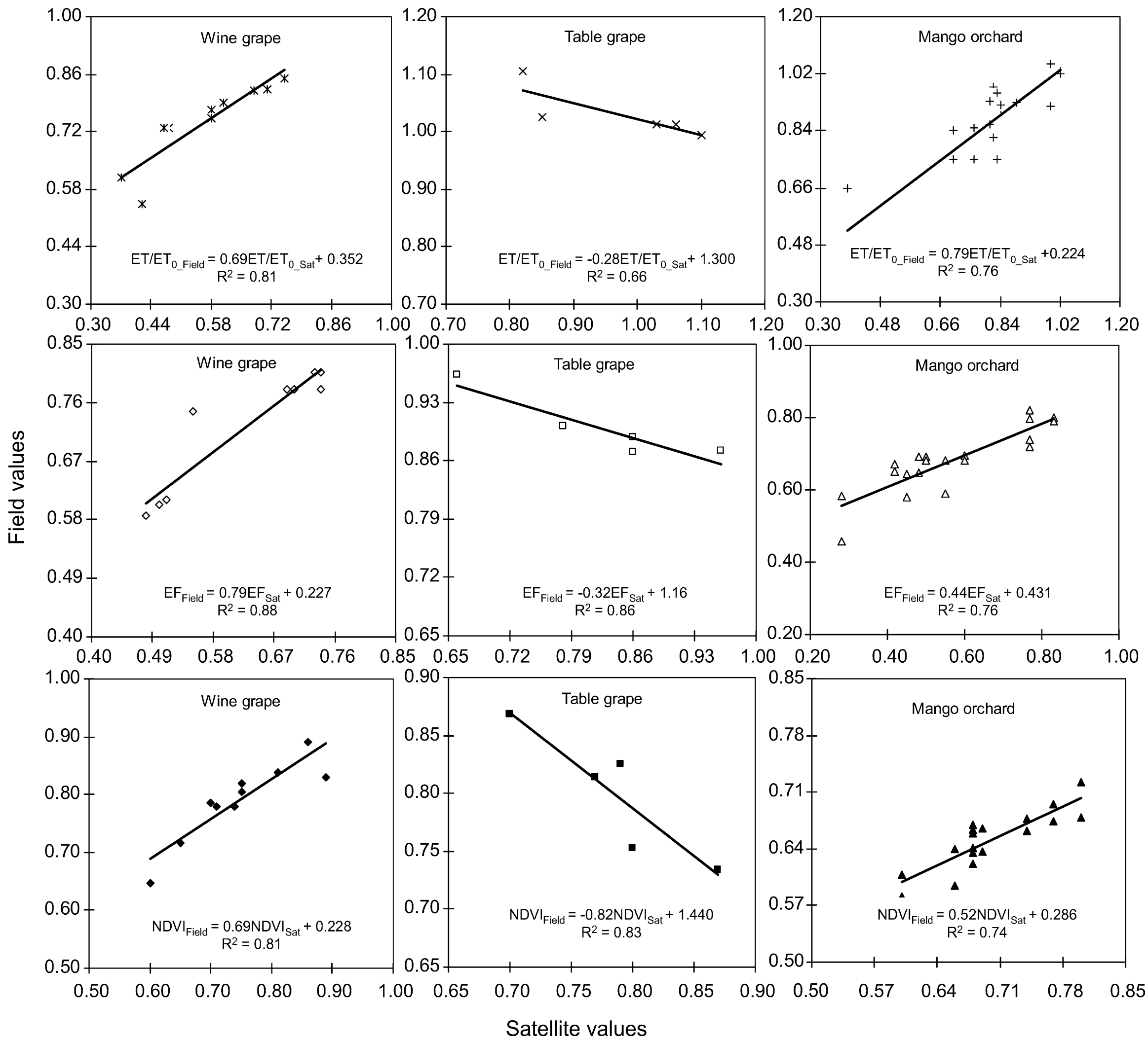

Fig. 10 – Relationship between field and satellite values of ET/ET0, EF and NDVI for irrigated crops. Values from images (subscript sat) involving the period from 2001 to 2007 were compared with field data of the growing seasons (subscript Field) of wine grape (2002), table grape (2003) and mango orchard (2003–2005) with the same DOY.

mance of the drip irrigation system. With the price of seedless grapes being 2.20 US\$ kg^{-1} in 2003, $CWP_{\$\_ET}$ ranged from 3.74 to 8.80 US\$ m^{-3}, providing more economic gross value of production than for wine grapes.

3.5.3. *Mangos*

The results of the crop water productivity analyses for mangos in Fruitfort farm are shown in Fig. 13. The bulk of the CWP_{ET} values for irrigated mango orchard are found between 2.20 and 3.80 kg m^{-3} in GS1 (95% of the pixels). The average value was 2.80 kg m^{-3} with a std of 0.88 kg m^{-3} (CV = 31%). For GS2, 97% of the pixels were found in the range between 3.40 and 5.00 kg m^{-3} averaging 4.00 kg m^{-3} with a std of 0.62 kg m^{-3} (CV = 16%). The seasonal averaged CV was lower than in the case of vineyards, showing more uniformity for Fruitfort farm. Considering the $T = f(ET)$ relationship obtained from the experimental plot (Teixeira et al., 2008a), and applying these curves to the entire farm, CWP_T became 2.82–4.86 kg m^{-3} for GS1 and 5.08 and 7.47 kg m^{-3} for GS2.

The main reason for the lower values of CWP found for GS1 could be ascribed to irrigation management during the rainy period. The farmer stopped irrigation for a too long time following rain showers. This caused some water stress. Considering the mango price of 1.02 US\$ kg^{-1} in 2005 and in the study region, the correspondent monetary crop water productivity values based on actual evapotranspiration ($CWP_{\$\_ET}$) varied between 2.24 and 5.10 US\$ m^{-3}.

Table 3 – Apparent harvest indices (AHI) obtained from farmer surveys and SEBAL-based biomass production.

Term	Unit	Wine grapes	Table grapes	Mango
Measured yield	kg ha^{-1}	6,183	11,200	44,999
Estimated BIO_{GS}	kg ha^{-1}	9,815	17,552	54,418
AHI	–	0.63	0.64	0.83

BIO_{GS}: Estimated biomass production for the growing seasons.

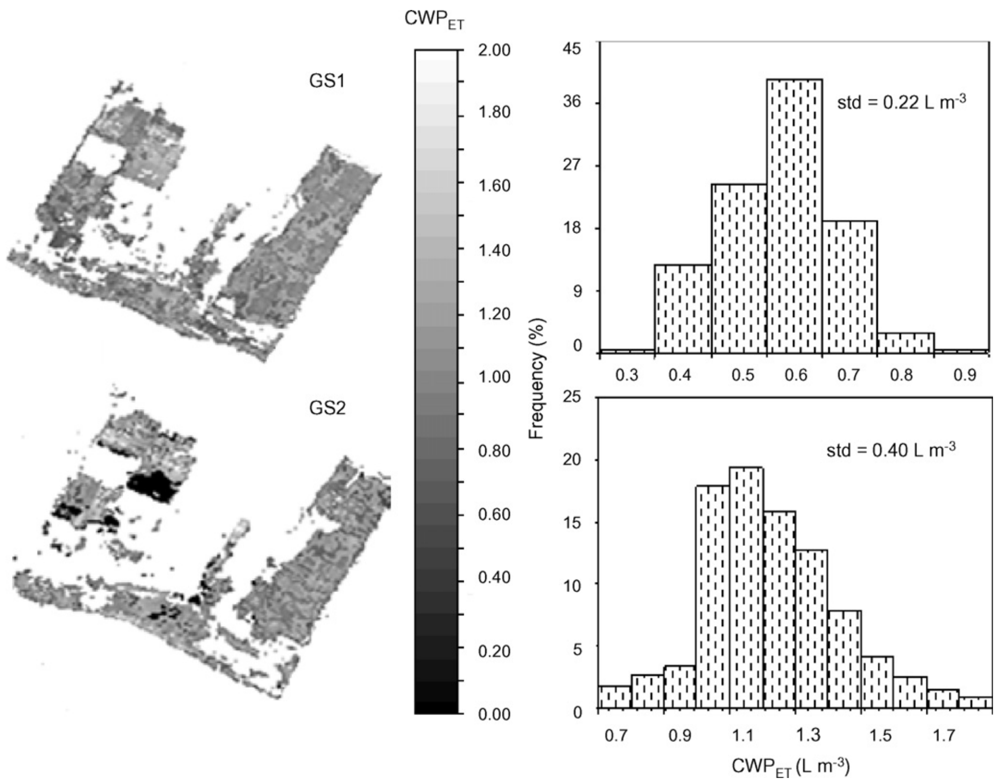

Fig. 11 – Crop water productivity based on actual evapotranspiration (CWP_{ET}) in Vitivinícola Santa Maria farm for the first (GS1) and second (GS2) growing seasons of wine grapes in 2002, Lagoa Grande, PE, Brazil.

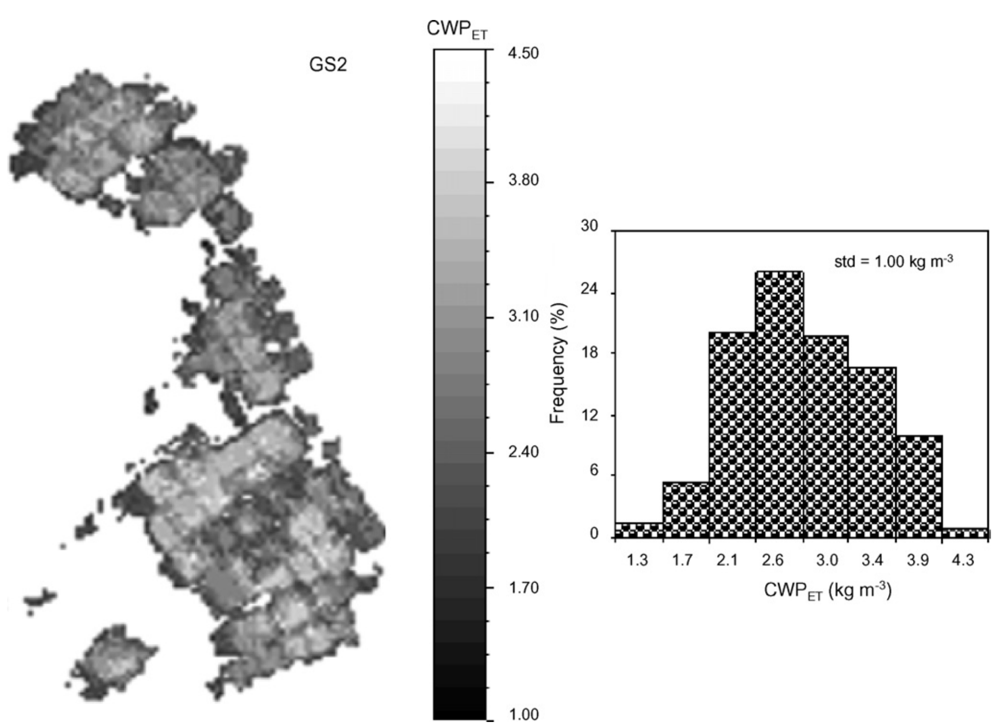

Fig. 12 – Crop water productivity based on actual evapotranspiration (CWP_{ET}) in Vale das Uvas Farm for the second growing season (GS2) of seedless table grapes in 2003, Petrolina, PE, Brazil.

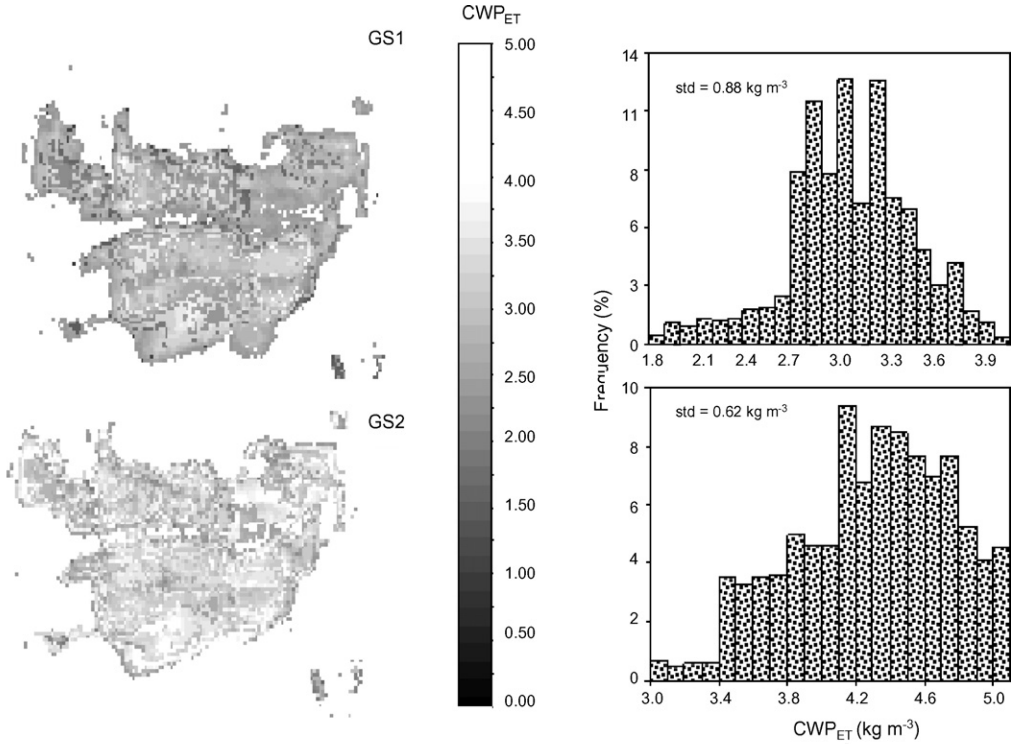

Fig. 13 – Crop water productivity based on CWP_{ET} in the Fruitfort Farm for the first (GS1) and second (GS2) growing seasons of mango orchard from 2003 to 2005, Petrolina, PE, Brazil.

Table 4 – Annual total crop water productivity parameters for vineyards and mango orchards: harvested area (HA); yield; crop water productivity per cultivated land (CWP_L); gross return (GR) and crop water productivity per actual evapotranspiration (CWP_{ET}, physical value; $CWP_{\$\_ET}$, monetary value) in Petrolina, PE, Brazil.

Irrigated crop	HA (ha)	Yield (t)	CWP_L (kg ha^{-1})	GR (US $)	CWP_{ET} (kg m^{-3})	$CWP_{\$\_ET}$ (US$ m^{-3})
Vineyards	3200	108,800	34,000	126,883	2.16	8.08
Mango orchards	6300	126,000	20,000	28,867	1.27	1.84

The averaged crop water productivity variables for vineyards (wine and table grapes together) and mango orchard in 2005 involving all producer farms in Petrolina, PE are summarized in Table 4. The values of CWP_{ET} for table grapes and mangos in Vale das Uvas and Fruitfort farms indicate a good performance, mainly in the case of the last farm. The lower economic value for table grapes in 2003 in relation to Table 4 is due to the increase in price in 2005 (3.04 US$ kg^{-1}). At a favourable market price, the gross margin of production for table grapes is order of magnitude higher than for wine grape. The overall production cost for the first vineyard is, however, significantly higher. Hence, the difference in net income between the two vineyards tends to decrease.

Economic water productivities from 2.50 to 7.50 US$ m^{-3} per unit of water depleted in table grapes and mango orchard are much higher than for irrigated annual crops. Sakthivadivel et al. (1999) reported typical values for arable crops to be 0.10–0.20 US$ m^{-3}. Further to that, orchards have intensive cultivation practices such as pruning and hand-picking, besides chemical protection and weed control. While large-scale arable crops such as wheat, maize, potatoes, soybean and cotton can be intensively mechanized, fruit cultivation require more labour.

4. Conclusions

The calibrated set of SEBAL equations have been applied to demonstrate that it is feasible to compute the changes in the energy and water balances when natural vegetation is being replaced by irrigated crops in Low-Middle São Francisco River basin. These are key information when Federal and Municipal Governments plan an expansion of the irrigated area. Regional water transfer plans in semi-arid region of Low-Middle São Francisco River basin are under preparation by the current Brazilian Federal Government, and the data analyzed in this study is highly relevant to apply concepts of evidence proofed decision making.

Using satellite images it was showed that the difference between SEBAL calculations and field measurements of accumulated actual evapotranspiration was less than 1% and 5% for irrigated mango orchard and caatinga ecosystems, respectively, when the equations are locally calibrated. These differences are lower than those reported in international SEBAL studies as a consequence of the local calibration processes. These accuracies are sufficient for further studies on the effect of land use changes on downstream river flow.

The satellite-based annual actual evapotranspiration for natural vegetation with an average of 500 mm is much lower than for mango orchards (1329 mm). Total withdrawal from river in Low-Middle São Francisco basin was estimated to be 1.25 $km^3\,year^{-1}$, total ET from irrigated land 1.22 $km^3\,year^{-1}$, incremental ET due to withdrawals 0.75 $km^3\,year^{-1}$, return flow 0.40 $km^3\,year^{-1}$, seepage to deep aquifers 0.10 $km\,year^{-1}$ and hence a net depletion of 0.85 $km^3\,year^{-1}$.

The total grape production in the Brazilian semi-arid region appeared to be lower than the average yield in other grape regions in the world. However, the annual production per hectare is comparable due to the multiple (2.5) growing seasons that are possible to achieve within one annual cycle. The bio-physical crop water productivities based on actual evapotranspiration (CWP_{ET}) in wine and table grapes averaged 0.80 $L\,m^3$ and 2.80 $kg\,m^{-3}$, respectively, while for mango orchard the mean value was 3.40 $kg\,m^{-3}$.

The analyses of economic water productivities in vineyards and mango orchards indicated that table grapes ranked the best (from 3.74 to 8.80 US$ m^{-3}), followed by mangos (from 2.24 to 5.10 $ m^{-3}) and wine grapes (from 0.36 to 1.55 $ m^{-3}). The agricultural water usage in the fruit farms is thus highly productive, and creates a considerable amount of jobs. Indeed, the towns of Petrolina, PE and Juazeiro, BA, in the semi-arid region of the Brazilian Northeast, have been growing in terms of exports and job creation, and these are good examples of converting marginal savannah land into booming rural developments. The irrigation management, however, requires full attention as significant percolation can adversely affect environments in terms of rising water tables and returning flow of polluted water to the river, being necessary more efficient water resources management for the expansion of irrigated areas.

REFERENCES

Allen, R.G., Pereira, L.S., Raes, D., Smith, M., 1998. Crop evapotranspiration. Guidelines for computing crop water requirements. FAO Irrigation and Drainage Paper 56, Rome, Italy, 300 pp.

Allen, R.G., Tasumi, M., Trezza, R., 2007a. Satellite-based energy balance for mapping evapotranspiration with internalized calibration (METRIC)—model. J. Irrig. Drain. Eng. ASCE 133 (4), 380–394.

Allen, R.G., Tasumi, M., Morse, A., Trezza, R., Wright, J.L., Bastiaanssen, W.G.M., Kramber, W., Lorite, I., Robison, C.W., 2007b. Satellite-based energy balance for mapping evapotranspiration with internalized calibration (METRIC)—applications. J. Irrig. Drain. Eng. ASCE 133, 395–406.

Asrar, G., Fuchs, M., Kanemasu, E.T., Hatfield, J.L., 1984. Estimating absorbed photosynthetically active radiation and leaf area index from spectral reflectance in wheat. Agron. J. 76, 300–306.

Bastiaansssen, W.G.M., 2000. SEBAL-based sensible and latent heat fluxes in the irrigated Gediz Basin, Turkey. J. Hydrol. 229, 87–100.

Bastiaansssen, W.G.M., Brito, R.A.L., Bos, M.G., Souza, R.A., Cavalcanti, E.B., Bakker, M.M., 2001. Low cost satellite data for monthly irrigation performance monitoring: benchmarks from Nilo Coelho, Brazil. Irrig. Drain. Syst. 15, 53–79.

Bastiaanssen, G.M.W., Chandrapala, L., 2003. Water balance variability across Sri Lanka for assessing agricultural and environmental water use. Agric. Water Manage. 58 (2), 171–192.

Bastiaanssen, W.G.M., Ali, S., 2003. A new crop yield forecasting model based on satellite measurements applied across the Indus Basin, Pakistan. Agric., Ecosyst. Environ. 94, 321–340.

Bastiaanssen, W.G.M., Noordman, E.J.M., Pelgrum, H., Davids, G., Allen, R.G., 2005. SEBAL for spatially distributed ET under actual management and growing conditions. J. Irrig. Drain. Eng. 131, 85–93.

Bastiaanssen, W.G.M., Binfang, W., Liping, J., Olson, D., 2008. The need for ET management of closed river basins with irrigated agriculture. In: WaterFront, World Water Council, Stockholm, Sweden (March 2008 issue).

Bos, M.G., Nugteren, J., 1974. On irrigation efficiencies. ILRI Publication No. 19. International Institute for Land Reclamation and Improvement (ILRI), Wageningen, The Netherlands, 138 pp.

Bos, M.G., Burton, D.J., Molden, D.J., 2005. Irrigation and Drainage Performance Assessment. Practical Guidelines. CABI Publishing, Cambridge, USA, 158 pp.

Droogers, P., Kite, G., 1999. Water productivity form integrated basin modeling. Irrig. Drain. Syst. 13 (3), 275–290.

Farah, H.O., Bastiaanssen, W.G.M., Feddes, R.A., 2004. Evaluation of the temporal variability of the evaporative fraction in a tropical watershed. Int. J. Appl. Earth Obs. Geoinf. 5, 129–140.

Field, C.B., Randerson, J.T., Malmstrfm, C.M., 1995. Global net primary production: combining ecology and remote sensing. Remote Sens. Environ. 51, 74–88.

Goodwin, M.G., O'Connell, 2008. Proceedings of the Vth International Symposium on Irrigation of Horticultural Crops. ISHS Acta Hort. 792 .

Jarmain, C., Klaasse, A., Bastiaanssen, W.G.M., Roux, A.S., 2007. Remote sensing tools for water use efficiency of grapes in the Winelands region, Western Cape. In: Proceedings of the 13th Sanciahs Symposium, Capetown, September 6–7, 2007.

Klaasse, A. Bastiaanssen, W.G.M., de Wit, M., Jarmain, C., Bosch, J., Roux, A., 2007. Satellite analysis of water use efficiency in the winelands region of Western Cape, South Africa, WaterWatch report for West Cape Department of Agriculture, Wageningen, The Netherlands, 70 pp.

Kustas, W.P., Norman, J.M., Schmugge, T.J., Anderson, M.C., 2004. Mapping surface energy fluxes with radiometric temperature. In: Quattrochi, D., Luvall, J. (Eds.), Thermal Remote Sensing in Land Surface Processes. CRC Press, Boca Raton, FL, USA.

Li, S.-G., Eugster, W., Asanuma, J., Kotani, A., Davaa, G., Oyunbaatar, D., Sugita, M., 2006. Energy partitioning and its biophysical controls above a grazing steppe in central Mongolia. Agric. Forest. Meteorol. 137, 89–106.

Monteith, J.L., 1972. Solar radiation and productivity in tropical ecosystems. J. Appl. Ecol. 9, 747–766.

Morse, A., Kramber, W.J., Allen, R.G., Tasumi, M., 2004. Use of the METRIC evapotranspiration model to compute water use by irrigated agriculture in Idaho. In: Proceedings of the International Geosciences and Remote Sensing Symposium, Anchorage, Alaska.

Oweis, T., Hachum, A., 2006. Water harvesting and supplemental irrigation for improved water productivity of dry farming systems in West Asia and North Africa. Agric. Water Manage. 80, 57–73.

Rockstrom, J., Barron, J., 2007. Water productivity in rainfed systems: overview of challenges and analysis of opportunities in water scarcity prone savannahs. Irrig. Sci. 25 (3), 299–311.

Sakthivadivel, R., de Fraiture, C., Molden, D.J., Perry, C., Kloezen, W., 1999. Indicators of land and water productivity in irrigated agriculture. Int. J. Water Res. Dev. 15, 161–180.

Steduto, P., Hsiao, T.C., Fereres, E., 2007. On the conservative behavior of biomass water productivity. Irrig. Sci. 25 (3), 189–207.

Teixeira, A.H.de.C., Bastiaanssen, W.G.M., Bassoi, L.H., 2007. Crop water parameters of irrigated wine and table grapes to support water productivity analysis in Sao Franciso river basin, Brazil. Agric. Water Manage. 94, 31–42.

Teixeira, A.H.de.C., Bastiaanssen, W.G.M., Ahmad, M.D., Moura, M.S.B., Bos, M.G., 2008a. Analysis of energy fluxes and vegetation-atmosphere parameters in irrigated and natural ecosystems of semi-arid Brazil. J. Hydrol. 362, 110–127.

Teixeira, A.H.de.C., Bastiaanssen, W.G.M., Moura, M.S.B., Soares, J.M., Ahmad, M.-ud-D., Bos, M.G., 2008b. Energy and water balance measurements for water productivity analysis in irrigated mango trees, Northeast Brazil. Agric. Forest. Meteorol. 148, 1524–1537.

Yunusa, I.A.M., Walker, R.R., Blackmore, D.H., 1997a. Characterization of water use by Sultana grapevines (*Vitis vinifera* L.) on their own roots or on Ramsey rootstock drip-irrigated with water of different salinities. Irrig. Sci. 17, 77–86.

Yunusa, I.A.M., Walker, R.R., Guy, J.R., 1997b. Portioning of seasonal evapotranspiration from a commercial furrow-irrigated Sultana vineyard. Irrig. Sci. 18, 45–54.

Walker, R., Gibberd, M., Stevens, R., Pech, J., 2004. Application of carbon isotopic discrimination technology to understand and managing wine grape water use efficiency. Final report to Grape and Wine Research and Development Corporation. Project Number CRV99/10.

Wolters, W., Bos, M.G., 1990. Irrigation performance assessment and irrigation efficiency. 1989 Annual report. International Institute for Land Reclamation and Improvement, Wageningen, The Netherlands.

Zwart, S.J., Bastiaanssen, W.G.M., 2004. Review of measured crop water productivity values for irrigated wheat, rice, cotton and maize. Agric. Water Manage. 69, 115–153.

Zwart, S., Bastiaanssen, W.G.M., 2007. SEBAL for detecting spatial variation of water productivity and scope for improvement in eight irrigated wheat systems. Agric. Water Manage. 89, 287–296.